

Published in final edited form as:

Development. 2007 June ; 134(11): 2137–2146. doi:10.1242/dev.002345.

Ena/VASP function in retinal axons is required for terminal arborization but not pathway navigation

Asha Dwivedy¹, Frank B. Gertler², Jeffrey Miller³, Christine E. Holt¹, and Cecile Lebrand^{4,*}

¹Department of Anatomy, University of Cambridge, Downing Street, Cambridge CB2 3DY, UK

²Department of Biology, Massachusetts Institute of Technology, Cambridge, MA 02139, USA

³Department of Genetics, Cell Biology and Development, University of Minnesota, Minneapolis, MN 55455, USA. ⁴Département de Biologie Cellulaire et de Morphologie, University of Lausanne, Rue de Bugnon, 9, 1005 Lausanne, Switzerland.

Abstract

The Enabled/vasodilator-stimulated phosphoprotein (Ena/VASP) family of proteins is required for filopodia formation in growth cones and plays a crucial role in guidance cue-induced remodeling of the actin cytoskeleton. In vivo studies with pharmacological inhibitors of actin polymerization have previously provided evidence for the view that filopodia are needed for growth cone navigation in the developing visual pathway. Here we have re-examined this issue using an alternative strategy to generate growth cones without filopodia in vivo by artificially targeting Xena/XVASP (*Xenopus* homologs of Ena/VASP) proteins to mitochondria in retinal ganglion cells (RGCs). We used the specific binding of the EVH1 domain of the Ena/VASP family of proteins with the ligand motif FP4 to sequester the protein at the mitochondria surface. RGCs with reduced function of Xena/XVASP proteins extended fewer axons out of the eye and possessed dynamic lamellipodial growth cones missing filopodia that advanced slowly in the optic tract. Surprisingly, despite lacking filopodia, the axons navigated along the optic pathway without obvious guidance errors, indicating that the Xena/XVASP family of proteins and filopodial protrusions are non-essential for pathfinding in retinal axons. However, depletion of Xena/XVASP proteins severely impaired the ability of growth cones to form branches within the optic tectum, suggesting that this protein family, and probably filopodia, plays a key role in establishing terminal arborizations.

Keywords

Ena/VASP; Filopodia; Branching; Guidance; Axon; Retina; *Xenopus*

Introduction

Growth cones select specific pathways that lead growing axons to their targets and this navigational ability is essential for establishing connections between neurons in the developing brain. Growth cone navigation involves the dynamic extension and withdrawal of actin-filled protrusions – filopodia – and experimental evidence suggests that these structures are important for steering axonal growth in response to guidance factors

*Author for correspondence (cecile.lebrand@unil.ch).

Supplementary material Supplementary material for this article is available at <http://dev.biologists.org/cgi/content/full/134/11/2137/DC1>

(Bovolenta and Mason, 1987; Davenport et al., 1993; Holt, 1989; Isbister and O'Connor, 2000; Mason and Wang, 1997; Myers and Bastiani, 1993; O'Connor et al., 1990; Zheng et al., 1996). The elimination of filopodia by treatment with cytochalasin, a drug that prevents actin filament elongation from barbed ends, causes misdirected axon growth in vivo in the developing vertebrate visual system (Chien et al., 1993) and in the developing grasshopper limb (Bentley and O'Connor, 1994).

The formation of filopodia and growth cone dynamics require continuous rearrangement of the actin and microtubule cytoskeleton (Lin and Forscher, 1995; Mallavarapu and Mitchison, 1999; Schaefer et al., 2002; Tanaka and Sabry, 1995; Zhou et al., 2002). Enabled/vasodilator-stimulated phosphoprotein (Ena/VASP) proteins are enriched at the tips of neuronal growth cone filopodia (Lanier et al., 1999) and have been shown to regulate the formation and the elongation of filopodia via actin dynamics (Lebrand et al., 2004). This family of proteins has been shown to contribute to axon guidance signaling in different species. *Drosophila ena* mutants have mild CNS defects and a 'bypass' phenotype of the intersegmental nerve (ISNb), which fails to branch in the appropriate regions (Gertler et al., 1995; Wills et al., 1999). Ena acts downstream of the Slit repulsive guidance factor by regulating the signal transduction of its receptor Robo (Bashaw et al., 2000). Similarly, genetic analysis in *Caenorhabditis elegans* identifies a function for the Ena homolog UNC-34 downstream of the attractive guidance receptor UNC-40/DCC for UNC-6/Netrin 1 as well as downstream of the repulsive guidance receptors UNC-5 for UNC-6/Netrin 1 and SAX-3/Robo for SLT-1/Slit (Colavita and Culotti, 1998; Gitai et al., 2003; Yu et al., 2002). In vertebrates, three Ena/VASP proteins exist: Mena, EVL (Ena/VASP-like) and VASP (Gertler et al., 1996). In mice, they are necessary for the appropriate guidance of commissural and sensory axons along the visual path (Lanier et al., 1999; Menzies et al., 2004). Netrin-1-induced filopodium formation is dependent upon the function of the Ena/VASP proteins and is directly correlated with their phosphorylation at a regulatory protein kinase A (PKA) site (Lebrand et al., 2004). These findings implicate a key role for the Ena/VASP proteins in the chemotropic responses of growth cones to guidance cues.

To investigate fully the role of the Ena/VASP proteins in growth cone dynamics and axon pathfinding in vivo, we used a sequestration strategy to block the function of all Ena/VASP family members – Xena, XVASP and XEVL – in the retinotectal system of *Xenopus* embryos. In brief, these proteins need to be localized adjacent to the plasma membrane in order to function in actin polymerization and have been rendered non-functional using an approach that instead targets them to the mitochondrial membrane (Bear et al., 2000). In contrast to previous genetic approaches that affect all cells, we have modified the activity of the Ena/VASP proteins in a subset of neurons, the retinal ganglion cells (RGCs) of the *Xenopus* retina. Using this approach, we confirmed that Xena/XVASP proteins play a fundamental role in the formation of growth cone filopodia in vivo. The lack of filopodia induced by the depletion of the Xena/XVASP proteins did not affect retinal axon pathfinding in vivo. However, depleted axons showed a reduced growth rate and longer pauses along the visual path. Strikingly, within the tectum, Ena/VASP protein knock-down drastically affected the branching of growing retinal axons. We thus propose that Xena/XVASP proteins control axonal growth cone dynamics, the speed of outgrowth and axonal branching by remodeling the actin network in response to guidance signals.

MATERIALS AND METHODS

Frog embryos

Fertilized eggs were obtained from hormone-induced mating of adult *Xenopus* females by in vitro fertilization. Embryos were dejellied in 2% cysteine (pH 8) and reared in 0.1× modified Barth's saline (MBS). Embryonic stages were determined according to Nieuwkoop

and Faber (Nieuwkoop and Faber, 1967). Motile embryos were anesthetized with 1.5 mM MS222 (Sigma, Germany) in 1× MBS before surgery or fixation.

Sequestration strategy specificity

We used the specific binding of the EVH1 domain of Ena/VASP proteins with the ligand motif DFPPPPXDE (abbreviated FP4) to sequester the Ena/VASP proteins (Bear et al., 2000). FP4-Mito expression in Rat2 fibroblasts and primary neurons removes all detectable Ena/VASP proteins from their normal site of localization at the cell plasma membrane and sequesters the proteins on the surface of mitochondria (Bear et al., 2000; Bear et al., 2002; Goh et al., 2002; Lebrand et al., 2004). In fibroblasts, it causes a phenotype identical to that of fibroblast lines that lack detectable Ena/VASP proteins. Expression of FP4-Mito induces no additional phenotypes in Ena/VASP-deficient fibroblasts, indicating that FP4-Mito-induced phenotypes in other cells most likely result from the inhibition of the function of the Ena/VASP proteins.

Plasmids and in vivo cDNA lipofection

Plasmid subcloning and PCR were performed using standard methods. The *FP4-Mito*-Green fluorescent protein (GFP) and *FP4-Mito*-Red fluorescent protein (RFP) constructs (Bear et al., 2000) were cloned into pCS2R plasmids for in vivo expression in *Xenopus*. Xena and XEVL have been cloned and described in great detail (Wanner et al., 2005; Xanthos et al., 2005). The RFP (Campbell et al., 2002) and GAP-GFP were cloned into pCS2R and used as generic controls and as markers to highlight the morphology of the retinal axons expressing the *Mito* constructs.

The constructs were introduced into all retinal precursor cells by pressure injecting the left eye primordia of stage 19 embryos with a mixture of the DNA construct and the lipofecting reagent DOTAP (Boehringer, Mannheim) at 1:3 weight:volume (w/v) (Holt et al., 1990; Lilienbaum et al., 1995). The embryos were transferred to 0.1× MBS and were allowed to grow for 44 hours (stage 33/34), 56-66 hours (stage 39/40) or 78-82 hours (41/42), depending on the experiments. RGCs were identified on the basis of layer position and cellular morphology. Retinas lipofected with the *Mito* constructs exhibited a similar organization to retinas expressing control constructs. Cells expressing the *Mito* constructs exhibited the entire range of differentiated retinal cell types and were not pycnotic, indicating that expression of the *FP4-Mito* construct does not interfere with the specification, migration, differentiation or short-term survival of retinal cells.

Cell culture

Retinal explant cultures were prepared from 33/34 embryos as described (Mann et al., 2002). After 40 hours, cells were fixed in 4% paraformaldehyde/phosphate-buffered saline (PBS) with 15% sucrose.

Imaging

Fixed and living samples were analyzed with a Nikon fluorescence microscope equipped with 10×, 20× or 40× Plan-NEOFLUAR objectives and 63×, 100× Plan-NEOFLUAR oil immersion objectives. Images were captured with an Orca-ER cooled CCD camera (Hamamatsu). All peripherals were controlled with Openlab software (Improvision). Z stacks of 15 images at 1 μm intervals, comprising the entire section thickness, were processed for deconvolution in Metamorph (Universal Imaging) and transferred to Photoshop software.

In vivo time-lapse video

At stage 39 or 42, embryos were anesthetized and the right optic tract and tectal area were exposed by removing carefully the right eye and skin as described (Chien et al., 1993). The heads of the embryos were mounted in a closed chamber containing freshly made 1× MBS, pH 7.4-7.5 containing 0.3 mM MS222. Heads were maintained at room temperature during the observation and were viable for as long as required (up to 12 hours).

Axons were observed with a 20× lens (Nikon Plan Apo, 0.75 NA), using adapted-epifluorescence filters connected to a standard 100W mercury lamp as well as neutral-density filters to reduce the illumination. To locate the position of the axon relative to brain landmarks, we captured low power (10×) bright-field and fluorescence pictures. For all movies, images were collected at 1 μm intervals in the z axis every 5, 15 or 30 minutes, depending on the experiment. Images from z-stack series of 15 images taken at the indicated intervals were de-convolved, compiled, aligned and converted into Quick-time movies with Metamorph.

Analysis

In vivo analysis of filopodial dynamics, elongation rate and stalling duration of retinal axon growth cones—A total of 15 GAP-GFP- and 15 GAP-GFP+FP4-Mito-RFP-expressing growth cones were analyzed at stage 39/40. Filopodial morphometric parameters were determined by measuring filopodial number and length every 30 minutes while the axons were growing from the ventral (VOT) to the dorsal optic tract (DOT) and at the tectal border. The average rate of axonal elongation was calculated from the time taken by axons to travel from the VOT to the DOT and to cross the tectal border. The average rate of axonal elongation represents a combination of the actual motion speed of intermittent displacement (basal rate of extension), and the frequency and duration of the intervening pauses. Growth cones were considered to be making a pause when they grew less than 10 μm in 20 minutes.

Analysis of axon elongation and pathfinding along the visual path—Analysis was made on fixed specimens because they allow measurement of a large number of axons. Trajectories of control and FP4-Mito-expressing RGC axons were analyzed at stage 33/34 in whole-mount retina, which permits us to follow the entire axons inside the eye (Holt, 1989). At stages 39 and 42, the trajectories of control and FP4-Mito-expressing axons were studied in 12 μm serial coronal cryostat sections from their origin in the retina to their tips in the tectum as well as in whole-mount brain preparations, as described (Holt, 1989; Riehl et al., 1996; Ruchhoeft et al., 1999). Different parameters were analyzed: polarization of the RGC axons in the retina as well as trajectories and the terminal point of each individual axon. In 12 μm serial sections of the retina, the number of ganglion cells expressing the RFP or FP4-Mito-GFP+RFP proteins was counted to give a total number of positive RGCs per retina. The point along the pathway where each positive-expressing axon ended (i.e. inside the eye, the brain entry point, the chiasm, the optic tract, tectum) was determined and then expressed as a percentage of the total number of positive RGCs. The percentages were an average of the counts made in ten embryos per condition and analyzed from three separate sets of experiments. Using appropriate statistical tests, the percentage values for FP4-Mito-GFP+RFP-expressing axons were compared to percentage values for RFP-expressing axons within the same animal, as well as from a different group of animals lipofected only with the RFP.

Branching analysis of retinal axons in vivo—The extent of axonal branching of stage 39/40 embryos was determined by measuring the branching of 20 control GAP-GFP- and 20 FP4-Mito-RFP+GAP-GFP-expressing retinal axons. Labeled axons were imaged at 5 or 15

minute intervals for a total observation period of at least 3 hours after the retinal axons had penetrated the tectum. All measurements were performed on images of reconstructed arbors taken every 30 minutes using Neurolucida software. The number and the length of the processes were defined as filopodia when they were less than 8 μm and as branches when they were greater than 8 μm . Branching development for each condition was analyzed by comparing parameters at time 0, 1, 2 and 3 hours after axons had entered the tectum. In addition, branching parameters of FP4-Mito-expressing axons was compared to branching parameters of control axons at similar times after tectal entry.

Statistical analysis—For all analysis, control and FP4-MITO values from at least three separate experiments were first tested for normality. Values that followed a normal distribution were compared using Student's *t*-test or one-way ANOVA and Fisher's *t*-tests. Values that did not follow a normal distribution were compared using Mann-Whitney and Kolmogorov-Smirnov non parametric tests.

RESULTS

Sequestering strategy depletes all Xena/XVASP proteins from axonal growth cones

Two members of the Ena/VASP family, Xena and XEVL, have been shown to be expressed in the *Xenopus* retina at the time when RCGs extend their axons (Wanner et al., 2005; Xanthos et al., 2005). To address the role of this family of proteins in RCG axonal pathfinding, we used a sequestering strategy that has been shown to neutralize specifically all three Ena/VASP proteins (Bear et al., 2000; Bear et al., 2002; Goh et al., 2002; Lebrand et al., 2004) (see Materials and methods). In brief, we used the very specific binding of the EVH1 domain of Ena/VASP proteins with the FP4 motif to deplete Ena/VASP proteins from the cell surface (Bear et al., 2000). By coupling four copies of the FP4 motif with a mitochondrial-targeting sequence ('*FP4-Mito*') all the endogenous Ena/VASP proteins were sequestered at the mitochondrial surface. A fusion of these constructs with the green fluorescent protein (*GFP*) sequence ('*FP4-Mito-GFP*') or with the red fluorescent protein (*RFP*) sequence ('*FP4-Mito-RFP*') allows a direct visualization of the targeted cells. In addition, simple vectors expressing the *RFP* or the *GFP* sequence fused to a plasma membrane-targeting motif (*GAP-GFP*) were used as lipofection controls and to visualize the morphology of cells and axons.

We first verified that the FP4-Mito construct is targeted to mitochondrial membrane (Fig. 1A-C) and that the sequestering strategy previously tested in mouse neurons operates in *Xenopus* RCGs. To this aim, we performed retinal co-transfection of the *FP4-Mito-RFP* plasmid with a construct encoding a fusion of the Xena protein gene sequence and *GFP* (*Xena-GFP*), and analyzed the cellular localization of the Xena-GFP protein in vivo (Fig. 1D-F) and in explants (Fig. 1G-L). Xena-GFP normally localized on the cell surface of RCGs. At growth cones, Xena-GFP punctate labeling was observed at the surface and was enriched at the tips of filopodia (Fig. 1G). By contrast, co-transfection of *Xena-GFP* with the *FP4-Mito-RFP* construct in retinal cells, from stage 34 to stage 42, showed Xena-GFP-positive staining typical of mitochondrial localization (Fig. 1D-F) (Bear et al., 2000; Lebrand et al., 2004). This RFP mitochondrial labeling correlates with a severe reduction of cell surface Xena-GFP staining, thereby confirming that the sequestering strategy efficiently depletes Xena-GFP proteins from the growth cones (Fig. 1J-L). Similar observations were made using XEVL-GFP (data not shown), indicating that all *Xenopus* Ena/VASP proteins present in retina are similarly sequestered by FP4-Mito on the mitochondria.

Xena/XVASP proteins regulate the morphology and dynamics of growth cone filopodia in vitro and in vivo

We next analyzed the effects of Xena/XVASP protein plasma membrane (PM) depletion on retinal axon growth cone morphology in vitro. Whereas control growth cones exhibited typical morphology, including the presence of lamellipodia and numerous filopodia (Fig. 1M,N), FP4-Mito-positive growth cones showed a drastic reduction in the number of filopodia (Fig. 1O). To investigate further how Xena/XVASP proteins regulate growth cone dynamics, we analyzed the behavior of individual retinal growth cones in vivo using time-lapse video microscopy in live *Xenopus* brains (Chien et al., 1993; Harris et al., 1987). GFP-positive control growth cones along the optic tract exhibited lamellipodial dynamics and rapid filopodial extension, exploration and withdrawal (Fig. 2A and see Movie 1 in the supplementary material). By contrast, the PM depletion of Xena/XVASP proteins induced, in vivo, a severe reduction in growth cone filopodial number, as observed previously in vitro. All along the optic tract and inside the tectum, retinal growth cones with reduced Xena/XVASP activity almost entirely lost their ability to form filopodia and frequently generated lamellipodia and ruffles (Fig. 2B and see Movie 2 in the supplementary material; and quantification Fig. 2C,D). Moreover, the few filopodia generated by Xena/XVASP-depleted growth cones were shorter than in control conditions. Therefore, Xena/XVASP function controls growth cone and filopodia dynamics in vitro and, more importantly, in vivo.

Depletion of Xena/XVASP proteins does not cause pathfinding errors along the visual pathway

To address the possibility that FP4-Mito expression interferes with the ability of RGC growth cones to navigate correctly inside the retina and brain, the trajectories of FP4-Mito-expressing axons were analyzed in detail on cryostat sections (Fig. 3) as well as in whole-mount retinas (data not shown) and brain preparations (Fig. 4). Pioneering retinal axons leave the eye at stage 28-29/30, cross the chiasm at stage 32, grow through the optic tract at stage 33/34-35/36 and arrive at the optic tectum at stage 37/38-40 (Dingwell et al., 2000). In the retina, from stage 33/34 to stage 42, FP4-Mito-expressing axons exhibited normal trajectories along the vitreal surface as well as in the optic nerve head (compare Fig. 3E,F with 3A,B). In control brains, at stage 39, numerous RGC axons had grown dorsally through the optic chiasm and the contralateral optic tract to innervate the optic tectum (Fig. 3A-D and Fig. 4A,B). By contrast, very few axons of neurons expressing the FP4-Mito construct were detected at stage 39 along the chiasm, the optic tract or in the tectum (Fig. 3G,H and Fig. 4C). However, the FP4-Mito-positive axons that did grow followed the normal visual pathway and did not stray into aberrant territories (compare Fig. 3G,H with 3C,D and Fig. 4C with 4B). The percentage of axons displaying guidance errors (axons with abrupt orientation changes or with extreme ventral or dorsal positions in the diencephalon) was identical in FP4-Mito-expressing and control retinal neurons (Figs 3, 4). With time-lapse video microscopy, we observed that growth cones of neurons expressing FP4-Mito followed normal paths and reached the tectum, their final target (Fig. 2B and see Movie 2 in the supplementary material). Thus, the absence of filopodia in neurons with depleted Xena/XVASP function does not interfere with the ability of growth cones to follow a normal route along the retinotectal pathway.

Xena/XVASP function interferes with axon elongation in the retina

In each control and FP4-Mito retina, on average 11 RGCs expressed the plasmid and the majority had an axon that could be followed at various distances along the visual pathway from the retina to the tectum. At stage 39, the majority of the RGCs expressing control constructs had initiated an axon ($79.8 \pm 5.5\%$), many of which had reached the optic tract and the tectum ($59.6 \pm 8.8\%$) (Fig. 3A, Fig. 5A). Similarly, nearly all FP4-Mito-expressing RGCs

had sent out an axon ($79.5 \pm 5.6\%$) (Fig. 3E). However, the distribution of their axonal tips along the visual pathways was significantly different from controls, because the majority of FP4-Mito-expressing axons remained inside the retina ($65.8 \pm 4.8\%$ compared with $33.9 \pm 9.4\%$ for controls, $P < 0.001$; Fig. 5A) and only few axons extended in the optic tract (Fig. 3H, Fig. 4C and Fig. 5A). Therefore, at stage 39, the majority of the axons of control neurons had already reached the tectum, whereas most of the FP4-Mito-expressing axons were still at the level of the optic nerve head in the retina. These results indicated that the PM depletion of Xena/XVASP proteins does not interfere with axon initiation but affects their extension, particularly within the eye.

To determine whether the inhibition of Xena/XVASP proteins completely halted or simply reduced the rate of axonal growth, the distribution of retinal axons along the optic pathway was studied at a second time point 48 hours later. At the latest stage (stage 42), the axons of the majority of the RGC neurons expressing either control (Fig. 3J) or FP4-Mito (Fig. 3K) constructs equally succeeded in reaching the tectum (Fig. 5A). Thus, Xena/XVASP PM depletion slowed the progression of retinal axons causing them to linger or stall in the visual pathway without affecting their capacity to reach their target.

Xena/XVASP function regulates the speed of axonal elongation in the retina and along the optic tract

To test the consequences of Xena/XVASP protein PM deletion on axonal outgrowth speed, we measured, *in vivo*, the rate of axon elongation as well as the duration of growth cone pauses by time-lapse video microscopy. Between the ventral and the dorsal optic tract, control growth cones exhibited filopodial dynamics and the axonal growth rate was $54 \mu\text{m}$ per hour (Fig. 5B). At the tectum entrance, axons significantly slowed down to an average speed of $30 \mu\text{m}$ per hour and became more complex, with filopodia-like processes extending in all directions, similar to previous findings (Harris et al., 1987).

By contrast, in FP4-Mito-expressing neurons, correlated to the drastic decrease of growth cone filopodia number, the average elongation rate of growth cones was significantly reduced compared with controls along the optic tract and at the tectal border (Fig. 5B). Instead of the steady forward motility observed in control axons, growth cones of FP4-Mito-expressing retinal neurons exhibited a significant decrease of their basal rate of extension and a significant increase in the duration of pauses in all regions of the optic tract and tectal border. The frequency of pauses was also increased in FP4-Mito-positive axons in the optic tract, but was about the same as controls at the border of the tectum. Some retinal growth cones that were observed to pause for several hours continued to exhibit active lamellipodial movement without forward advance (see Fig. S1 in the supplementary material). These results indicate that the function of Xena/XVASP proteins controls the speed of axonal elongation and the pause time of growth cones.

Xena/XVASP proteins control the branching of retinotectal axons

Finally, we studied the formation of the retinotectal axon terminal arborizations *in vivo*. Axonal arbors were imaged by time-lapse video microscopy at 15 minute intervals during periods lasting for 3 to 12 hours. Soon after control axons had entered the tectum, they made pauses and extended numerous filopodia. We observed filopodia-mediated branching at the growth cone and on the axonal shaft (Fig. 6A and see Movie 3 in the supplementary material) (see also Harris et al., 1987). By contrast, pausing FP4-Mito-expressing retinal axons exhibited a drastic reduction in filopodial activity, as well as in branch formation, after they penetrated the tectum, and this lasted for the whole recording period of 12 hours (Fig. 6B and see Movie 4 in the supplementary material). Unlike control axons, which made sharp turns, these axons followed a straight path within the tectum.

To analyze and quantify the observed branching defects, axonal terminal arborizations were reconstructed using images collected every 30 minutes during the 3 hours following the entry of retinal axons into the tectum (Fig. 6C,D). In controls, the numbers of primary, or secondary, branch segments and of total branch segments, the number of nodes and the length of the total arborization all increased during the 3 hours of recording (Fig. 6C and Fig. 7). The significant increase of total arborization during the first hour was due to an increase in the number of branches, because the average length of the branch segments did not change significantly during the recording period. During the last two hours, although new primary and secondary branches were generated, the total length of the arbors remained relatively constant, because branch formation was counterbalanced by branch retraction.

By contrast, after Xena/XVASP protein depletion, the number of primary or secondary branch segments, of total branch segments, of nodes and the total length of the axon terminal arborizations did not significantly increase compared to the starting point (Fig. 6D and Fig. 7). At all time points, the expression of FP4-Mito significantly impaired all these parameters compared with controls. These neurons lost the capacity to branch, because they only generated very few primary branches and never formed secondary nor tertiary branches. However, the average length of branch segments of FP4-Mito-expressing axons, at all times, was unchanged as compared with the length of control branches. This indicated that Xena/XVASP activity regulated the elaboration of new branches and not the elongation of existing branches. These observations underscore the involvement of Xena/XVASP proteins in regulating the building of retinotectal axon arborizations.

DISCUSSION

Our time-lapse video-microscopy study in intact *Xenopus* brains investigates in vivo, for the first time, the specific functions of the Ena/VASP proteins in regulating growth cone and filopodial dynamics, and their consequences in the development of the retinotectal pathway. Surprisingly, the drastic decrease in the number of filopodia on retinal growth cones following Xena/XVASP depletion did not cause detectable axonal guidance mistakes along the visual pathway. However, the dynamics of retinotectal pathway formation and its branching pattern was significantly altered in axons affected by Xena/XVASP PM depletion. The average rate of axonal outgrowth was found to be severely reduced, especially at two crucial choice points for axonal guidance – the eye exit and the tectal border – due to reduced basal rates of extension and extended pauses of the growth cones in the absence of filopodia. In the tectum, we found that filopodial activity was required for the elaboration of new axonal branches. This study highlights the involvement of the function of the Ena/VASP proteins and filopodial dynamics in regulating axonal outgrowth, branching and terminal arborization in vivo.

Ena/VASP proteins regulate the actin cytoskeleton dynamics of growth cones

Our current study in *Xenopus* embryos shows that Ena/VASP activity is directly correlated with the capacity of retinal axon growth cones to generate and extend filopodia. This in vivo study confirms our previous work on cultured primary hippocampal neurons showing that growth cones with impaired Ena/VASP function lost almost all their ability to form filopodia but frequently developed large lamellipodia with ruffles (Lebrand et al., 2004). These effects were found to result principally from the reduced capacity of growth cones, in the absence of Ena/VASP proteins, to form the actin filament bundles that comprise filopodia, as well as from the increase in the density of networks of short actin filament at the lamellipodia leading edge (Lebrand et al., 2004).

Biochemical experiments indicate that Ena/VASP proteins facilitate actin filament assembly within cells by acting as ‘anti-capping’ proteins (Barzik et al., 2005; Bear et al., 2002). After

binding at the barbed ends of growing actin filaments, Ena/VASP proteins facilitate continued elongation of these filaments by protecting them from the activity of capping proteins, which stop the polymerization. The anti-capping activity of the Ena/VASP proteins could facilitate the elongation of the privileged filaments that constitute nascent filopodia. In addition, Ena/VASP proteins may play a direct role in actin filament elongation via their ability to reduce the branching of actin filaments as well as their action on the bundling of actin filaments (Barzik et al., 2005; Gertler et al., 1996; Huttelmaier et al., 1999; Krause et al., 2003; Lambrechts et al., 2000; Niebuhr et al., 1997; Reinhard et al., 1992; Skoble et al., 2001; Walders-Harbeck et al., 2002).

Ena/VASP and axonal guidance

Whereas Ena/VASP inhibition induces a drastic reduction of growth cone filopodial dynamics, it does not cause any major pathfinding defects of retinal axons along the visual pathway. The absence of pathfinding defects is surprising, because numerous *in vitro* and *in vivo* studies have previously indicated a major contribution of growth cone filopodia to axon guidance. Filopodia are considered as sensory structures at the tips of growth cones that coordinate the first responses to guidance signals (Bovolenta and Mason, 1987; Davenport et al., 1993; Dingwell et al., 2000; Holt, 1989; Isbister and O'Connor, 2000; Mason and Wang, 1997; Myers and Bastiani, 1993; O'Connor et al., 1990; Sabry et al., 1991; Zheng et al., 1996). The use of cytochalasin, a drug that disrupts the actin filaments of filopodia, shows that they are not required for growth cone advance but are indispensable for growth cone steering *in vitro* (Marsh and Letourneau, 1984; Zheng et al., 1996). More importantly, when filopodial formation is inhibited by cytochalasin treatment *in vivo*, the axons do not orient properly and follow abnormal pathways (Bentley and O'Connor, 1994; Chien et al., 1993). Time-lapse experiments in *Xenopus* indicate that cytochalasin-treated retinal growth cones lacking filopodia slow down and fail to reach the tectum (Chien et al., 1993).

Why do the filopodia-less growth cones in the current study fail to show this phenotype? The experiments with cytochalasin treatment must be interpreted with caution because this drug interferes with the organization of the actin cytoskeleton of all cell compartments. Therefore, cellular functions other than just filopodial dynamics may be affected. This includes mRNA trafficking and translation as well as membrane trafficking, endocytosis and degradation, processes that are important for directed axon outgrowth (Campbell and Holt, 2001; Ellis and Mellor, 2000; Lee and De Camilli, 2002; Merrifield et al., 1999; Murphy et al., 1996; Ochoa et al., 2000; Qualmann et al., 2000; Qualmann and Kessels, 2002; Salazar et al., 2003; Taunton et al., 2000; van Horck et al., 2004). In the current study, only filopodial dynamics were affected while other functions remained unchanged.

Our results are consistent with a recent study reporting that interfering genetically with Ena (UNC-34) function in *C. elegans* affects the dynamics of lamellipodia and filopodia but does not result in axonal pathfinding defects (Chang et al., 2006). In addition, in *Xenopus* embryos, expression of a dominant-negative Cdc42 construct by retinal axons reduces the number and length of filopodia on growth cones, but does not cause targeting errors (Ruchhoeft et al., 1999). In *Drosophila*, *in vivo* time-lapse microscopy suggests that growth cone pathfinding and filopodial dynamics are independently regulated by Cdc42 activation (Kim et al., 2002).

Retinal growth cones without filopodia might find their appropriate pathways by using other strategies for axonal guidance. In the *Xenopus* visual system, growth cones respond to long-range cues acting via a diffusion gradient or to local short-range cues that include cell-cell interactions (Brittis et al., 1995; Dingwell et al., 2000; Tessier-Lavigne and Goodman, 1996). Thus, retinal axon growth cones without filopodia after impaired Ena/VASP function could use mechanisms of contact adhesion or contact repulsion in order to follow their

appropriate paths. In our work, unlike in cytochalasin experiments, not all RGCs express the Ena/VASP-interfering construct. Therefore, some pioneer axons are preserved and, because they elongate at higher rate, they will lead in front of the axons with reduced Ena/VASP function. The retinal axon growth cones of the latter could also use adhesion mechanisms to follow the intact pioneer axons.

Genetic analyses in mice have shown that expression of the Ena/VASP proteins is required for the formation of specific axon pathways (Lanier et al., 1999; Menzies et al., 2004). Because Ena/VASP proteins are extensively expressed in all neurons as well as glial cells of the CNS, the axonal pathway defects observed in mutant mice may be caused by the absence of Ena/VASP activity in neurons, in glia, or in both. In our work, at variance to the genetic approach, the activity of Ena/VASP proteins is impaired in a subset of retinal ganglion cells and not in the cells of the entire animal. This strategy, as well as differences between species, may explain the absence of the mis-targeting phenotype observed in our experimental conditions compared with knock-out mice.

Ena/VASP proteins, axonal outgrowth and branching

The present study indicates that Ena/VASP depletion autonomously regulates the rate of retinal axon elongation, as well as growth cone pauses at the retina exit and along the optic tract. These results indicate that, whereas filopodia are not required for the retinal growth cones to find their appropriate paths, they are necessary for the axon to grow at the appropriate speed. Our observations of retinal growth cones that exhibit active lamellipodial movement without forward advance corroborate with the study by D. Goldberg's group showing that, as compared to laminin substrate, growth cones on polysine have a predominant lamellar morphology and slower motion (Rivas et al., 1992). The capacity of growth cones to sense with their filopodia long-range cues such as gradients of Netrin 1, Slit1, Slit2 and Ephrins localized along the visual paths may constitute an additional mechanism for the axons to respond quickly and appropriately at decision points (de la Torre et al., 1997; Deiner et al., 1997; Dingwell et al., 2000; Hutson and Chien, 2002; Plump et al., 2002). Ena/VASP are known to act downstream of Abl and the axon guidance receptors Robo, DCC and UNC-5 in vertebrates, *Drosophila* and *C. elegans* (Bashaw et al., 2000; Colavita and Culotti, 1998; Gertler et al., 1995; Gitai et al., 2003; Wills et al., 1999; Yu and Bargmann, 2001). Thus, in the absence activity of the Ena/VASP proteins, the guidance signaling responses to these cues may be blocked, resulting in longer pauses and forcing the growth cones to find their route using less-efficient compensatory mechanisms.

This study in *Xenopus* embryos has highlighted the crucial function of Ena/VASP proteins in regulating retinal axon terminal branching inside the tectum. The development of the *Xenopus* retinotectal arborization is dependent on different cellular mechanisms that regulate the formation of new branches or the equilibrium between extension, retraction and elimination of existing branches (Ruthazer and Cline, 2004; Sin et al., 2002; Witte et al., 1996). Our data indicate that Ena/VASP proteins promote the addition of new branches but do not regulate the length of existing branches. These results are in accordance with previous observations made on primary dissociated hippocampal neurons (Lebrand et al., 2004). Studies on the branching of cortical neurons or dendritic trees of Purkinje cells have shown that a branch often begins as a single filopodium and that initiation of axon branching requires both dynamic microtubules and actin filaments (Berry and Bradley, 1976a; Berry and Bradley, 1976b; Dent et al., 1999; Dent et al., 2003; Dent and Kalil, 2001). Thus, Ena/VASP proteins, by regulating actin filament elongation in filopodia localized at the growth cone or along the axonal shaft, are good candidates for the regulation of the elaboration of new branches. These results suggest strongly that, after Ena/VASP inactivation, the final targeting of retinal axons inside the tectum may be impaired, a topic of major interest for future investigations.

Supplementary Material

Refer to Web version on PubMed Central for supplementary material.

Acknowledgments

We thank members of the C. E. Holt and B. Harris's laboratories for helpful discussion. We particularly thank J-P. Hornung, S. Garel, P. Gaspar and P. Clarke for the reading of and comments on the manuscript. This work was supported by institutional research funds of the DBCM to C.L.; by Wellcome Trust Programme Grant to C.E.H.; and NIH grant GM68678 and CMI collaborative grant to F.B.G.

References

- Barzik M, Kotova TI, Higgs HN, Hazelwood L, Hanein D, Gertler FB, Schafer DA. Ena/VASP proteins enhance actin polymerization in the presence of barbed end capping proteins. *J. Biol. Chem.* 2005; 280:28653–28662. [PubMed: 15939738]
- Bashaw GJ, Kidd T, Murray D, Pawson T, Goodman CS. Repulsive axon guidance: Abelson and Enabled play opposing roles downstream of the roundabout receptor. *Cell.* 2000; 101:703–715. [PubMed: 10892742]
- Bear JE, Loureiro JJ, Libova I, Fassler R, Wehland J, Gertler FB. Negative regulation of fibroblast motility by Ena/VASP proteins. *Cell.* 2000; 101:717–728. [PubMed: 10892743]
- Bear JE, Svitkina TM, Krause M, Schafer DA, Loureiro JJ, Strasser GA, Maly IV, Chaga OY, Cooper JA, Borisy GG, et al. Antagonism between Ena/VASP proteins and actin filament capping regulates fibroblast motility. *Cell.* 2002; 109:509–521. [PubMed: 12086607]
- Bentley D, O'Connor TP. Cytoskeletal events in growth cone steering. *Curr. Opin. Neurobiol.* 1994; 4:43–48. [PubMed: 8173324]
- Berry M, Bradley P. The growth of the dendritic trees of Purkinje cells in irradiated agranular cerebellar cortex. *Brain Res.* 1976a; 116:361–387. [PubMed: 974782]
- Berry M, Bradley P. The growth of the dendritic trees of Purkinje cells in the cerebellum of the rat. *Brain Res.* 1976b; 112:1–35. [PubMed: 947479]
- Bovolenta P, Mason C. Growth cone morphology varies with position in the developing mouse visual pathway from retina to first targets. *J. Neurosci.* 1987; 7:1447–1460. [PubMed: 3572487]
- Brittis PA, Lemmon V, Rutishauser U, Silver J. Unique changes of ganglion cell growth cone behavior following cell adhesion molecule perturbations: a time-lapse study of the living retina. *Mol. Cell. Neurosci.* 1995; 6:433–449. [PubMed: 8581314]
- Campbell DS, Holt CE. Chemotropic responses of retinal growth cones mediated by rapid local protein synthesis and degradation. *Neuron.* 2001; 32:1013–1026. [PubMed: 11754834]
- Campbell RE, Tour O, Palmer AE, Steinbach PA, Baird GS, Zacharias DA, Tsien RY. A monomeric red fluorescent protein. *Proc. Natl. Acad. Sci. USA.* 2002; 99:7877–7882. [PubMed: 12060735]
- Chang C, Adler CE, Krause M, Clark SG, Gertler FB, Tessier-Lavigne M, Bargmann CI. MIG-10/lamellipodin and AGE-1/PI3K promote axon guidance and outgrowth in response to slit and netrin. *Curr. Biol.* 2006; 16:854–862. [PubMed: 16618541]
- Chien CB, Rosenthal DE, Harris WA, Holt CE. Navigational errors made by growth cones without filopodia in the embryonic *Xenopus* brain. *Neuron.* 1993; 11:237–251. [PubMed: 8352941]
- Colavita A, Culotti JG. Suppressors of ectopic UNC-5 growth cone steering identify eight genes involved in axon guidance in *Caenorhabditis elegans*. *Dev. Biol.* 1998; 194:72–85. [PubMed: 9473333]
- Davenport RW, Dou P, Rehder V, Kater SB. A sensory role for neuronal growth cone filopodia. *Nature.* 1993; 361:721–724. [PubMed: 8441465]
- de la Torre JR, Hopker VH, Ming GL, Poo MM, Tessier-Lavigne M, Hemmati-Brivanlou A, Holt CE. Turning of retinal growth cones in a netrin-1 gradient mediated by the netrin receptor DCC. *Neuron.* 1997; 19:1211–1224. [PubMed: 9427245]
- Deiner MS, Kennedy TE, Fazeli A, Serafini T, Tessier-Lavigne M, Sretavan DW. Netrin-1 and DCC mediate axon guidance locally at the optic disc: loss of function leads to optic nerve hypoplasia. *Neuron.* 1997; 19:575–589. [PubMed: 9331350]

- Dent EW, Kalil K. Axon branching requires interactions between dynamic microtubules and actin filaments. *J. Neurosci.* 2001; 21:9757–9769. [PubMed: 11739584]
- Dent EW, Callaway JL, Szebenyi G, Baas PW, Kalil K. Reorganization and movement of microtubules in axonal growth cones and developing interstitial branches. *J. Neurosci.* 1999; 19:8894–8908. [PubMed: 10516309]
- Dent EW, Tang F, Kalil K. Axon guidance by growth cones and branches: common cytoskeletal and signaling mechanisms. *Neuroscientist.* 2003; 9:343–353. [PubMed: 14580119]
- Dingwell KS, Holt CE, Harris WA. The multiple decisions made by growth cones of RGCs as they navigate from the retina to the tectum in *Xenopus* embryos. *J. Neurobiol.* 2000; 44:246–259. [PubMed: 10934326]
- Ellis S, Mellor H. Regulation of endocytic traffic by rho family GTPases. *Trends Cell Biol.* 2000; 10:85–88. [PubMed: 10675900]
- Gertler FB, Comer AR, Juang JL, Ahern SM, Clark MJ, Liebl EC, Hoffmann FM. Enabled, a dosage-sensitive suppressor of mutations in the *Drosophila* Abl tyrosine kinase, encodes an Abl substrate with SH3 domain-binding properties. *Genes Dev.* 1995; 9:521–533. [PubMed: 7535279]
- Gertler FB, Niebuhr K, Reinhard M, Wehland J, Soriano P. Mena, a relative of VASP and *Drosophila* Enabled, is implicated in the control of microfilament dynamics. *Cell.* 1996; 87:227–239. [PubMed: 8861907]
- Gitai Z, Yu TW, Lundquist EA, Tessier-Lavigne M, Bargmann CI. The netrin receptor UNC-40/DCC stimulates axon attraction and outgrowth through Enabled and, in parallel, Rac and UNC-115/AbLIM. *Neuron.* 2003; 37:53–65. [PubMed: 12526772]
- Goh KL, Cai L, Cepko CL, Gertler FB. Ena/VASP proteins regulate cortical neuronal positioning. *Curr. Biol.* 2002; 12:565–569. [PubMed: 11937025]
- Harris WA, Holt CE, Bonhoeffer F. Retinal axons with and without their somata, growing to and arborizing in the tectum of *Xenopus* embryos: a time-lapse video study of single fibres in vivo. *Development.* 1987; 101:123–133. [PubMed: 3449363]
- Holt CE. A single-cell analysis of early retinal ganglion cell differentiation in *Xenopus*: from soma to axon tip. *J. Neurosci.* 1989; 9:3123–3145. [PubMed: 2795157]
- Holt CE, Garlick N, Cornel E. Lipofection of cDNAs in the embryonic vertebrate central nervous system. *Neuron.* 1990; 4:203–214. [PubMed: 1689586]
- Hutson LD, Chien CB. Pathfinding and error correction by retinal axons: the role of *astray/robo2*. *Neuron.* 2002; 33:205–217. [PubMed: 11804569]
- Huttelmaier S, Harbeck B, Steffens O, Messerschmidt T, Illenberger S, Jockusch BM. Characterization of the actin binding properties of the vasodilator-stimulated phosphoprotein VASP. *FEBS Lett.* 1999; 451:68–74. [PubMed: 10356985]
- Isbister CM, O'Connor TP. Mechanisms of growth cone guidance and motility in the developing grasshopper embryo. *J. Neurobiol.* 2000; 44:271–280. [PubMed: 10934328]
- Kim MD, Kolodziej P, Chiba A. Growth cone pathfinding and filopodial dynamics are mediated separately by Cdc42 activation. *J. Neurosci.* 2002; 22:1794–1806. [PubMed: 11880508]
- Krause M, Dent EW, Bear JE, Loureiro JJ, Gertler FB. Ena/VASP proteins: regulators of the actin cytoskeleton and cell migration. *Annu. Rev. Cell Dev. Biol.* 2003; 19:541–564. [PubMed: 14570581]
- Lambrechts A, Kwiatkowski AV, Lanier LM, Bear JE, Vandekerckhove J, Ampe C, Gertler FB. cAMP-dependent protein kinase phosphorylation of EVL, a Mena/VASP relative, regulates its interaction with actin and SH3 domains. *J. Biol. Chem.* 2000; 275:36143–36151. [PubMed: 10945997]
- Lanier LM, Gates MA, Witke W, Menzies AS, Wehman AM, Macklis JD, Kwiatkowski D, Soriano P, Gertler FB. Mena is required for neurulation and commissure formation. *Neuron.* 1999; 22:313–325. [PubMed: 10069337]
- Lebrand C, Dent EW, Strasser GA, Lanier LM, Krause M, Svitkina TM, Borisy GG, Gertler FB. Critical role of Ena/VASP proteins for filopodia formation in neurons and in function downstream of netrin-1. *Neuron.* 2004; 42:37–49. [PubMed: 15066263]
- Lee E, De Camilli P. Dynamin at actin tails. *Proc. Natl. Acad. Sci. USA.* 2002; 99:161–166. [PubMed: 11782545]

- Lilienbaum A, Reszka AA, Horwitz AF, Holt CE. Chimeric integrins expressed in retinal ganglion cells impair process outgrowth in vivo. *Mol. Cell. Neurosci.* 1995; 6:139–152. [PubMed: 7551566]
- Lin CH, Forscher P. Growth cone advance is inversely proportional to retrograde F-actin flow. *Neuron.* 1995; 14:763–771. [PubMed: 7536426]
- Mallavarapu A, Mitchison T. Regulated actin cytoskeleton assembly at filopodium tips controls their extension and retraction. *J. Cell Biol.* 1999; 146:1097–1106. [PubMed: 10477762]
- Mann F, Ray S, Harris W, Holt C. Topographic mapping in dorsoventral axis of the *Xenopus* retinotectal system depends on signaling through ephrin-B ligands. *Neuron.* 2002; 35:461–473. [PubMed: 12165469]
- Marsh L, Letourneau PC. Growth of neurites without filopodial or lamellipodial activity in the presence of cytochalasin B. *J. Cell Biol.* 1984; 99:2041–2047. [PubMed: 6389568]
- Mason CA, Wang LC. Growth cone form is behavior-specific and, consequently, position-specific along the retinal axon pathway. *J. Neurosci.* 1997; 17:1086–1100. [PubMed: 8994063]
- Menzies AS, Aszodi A, Williams SE, Pfeifer A, Wehman AM, Goh KL, Mason CA, Fassler R, Gertler FB. Mena and vasodilator-stimulated phosphoprotein are required for multiple actin-dependent processes that shape the vertebrate nervous system. *J. Neurosci.* 2004; 24:8029–8038. [PubMed: 15371503]
- Merrifield CJ, Moss SE, Ballestrem C, Imhof BA, Giese G, Wunderlich I, Almers W. Endocytic vesicles move at the tips of actin tails in cultured mast cells. *Nat. Cell Biol.* 1999; 1:72–74. [PubMed: 10559868]
- Murphy C, Saffrich R, Grummt M, Gournier H, Rybin V, Rubino M, Auvinen P, Lutcke A, Parton RG, Zerial M. Endosome dynamics regulated by a Rho protein. *Nature.* 1996; 384:427–432. [PubMed: 8945468]
- Myers PZ, Bastiani MJ. Growth cone dynamics during the migration of an identified commissural growth cone. *J. Neurosci.* 1993; 13:127–143. [PubMed: 8423468]
- Niebuhr K, Ebel F, Frank R, Reinhard M, Domann E, Carl UD, Walter U, Gertler FB, Wehland J, Chakraborty T. A novel proline-rich motif present in ActA of *Listeria monocytogenes* and cytoskeletal proteins is the ligand for the EVH1 domain, a protein module present in the Ena/VASP family. *EMBO J.* 1997; 16:5433–5444. [PubMed: 9312002]
- Nieukoop, PD.; Faber, J. *Normal Table of Xenopus laevis* (Daudin). North Holland; Amsterdam: 1967.
- O'Connor TP, Duerr JS, Bentley D. Pioneer growth cone steering decisions mediated by single filopodial contacts in situ. *J. Neurosci.* 1990; 10:3935–3946. [PubMed: 2269892]
- Ochoa GC, Slepnev VI, Neff L, Ringstad N, Takei K, Daniell L, Kim W, Cao H, McNiven M, Baron R, et al. A functional link between dynamin and the actin cytoskeleton at podosomes. *J. Cell Biol.* 2000; 150:377–389. [PubMed: 10908579]
- Plump AS, Erskine L, Sabatier C, Brose K, Epstein CJ, Goodman CS, Mason CA, Tessier-Lavigne M. Slit1 and Slit2 cooperate to prevent premature midline crossing of retinal axons in the mouse visual system. *Neuron.* 2002; 33:219–232. [PubMed: 11804570]
- Qualmann B, Kessels MM. Endocytosis and the cytoskeleton. *Int. Rev. Cytol.* 2002; 220:93–144. [PubMed: 12224553]
- Qualmann B, Kessels MM, Kelly RB. Molecular links between endocytosis and the actin cytoskeleton. *J. Cell Biol.* 2000; 150:F111–F116. [PubMed: 10974009]
- Reinhard M, Halbrugge M, Scheer U, Wiegand C, Jockusch BM, Walter U. The 46/50 kDa phosphoprotein VASP purified from human platelets is a novel protein associated with actin filaments and focal contacts. *EMBO J.* 1992; 11:2063–2070. [PubMed: 1318192]
- Riehl R, Johnson K, Bradley R, Grunwald GB, Cornel E, Lilienbaum A, Holt CE. Cadherin function is required for axon outgrowth in retinal ganglion cells in vivo. *Neuron.* 1996; 17:837–848. [PubMed: 8938117]
- Rivas RJ, Burmeister DW, Goldberg DJ. Rapid effects of laminin on the growth cone. *Neuron.* 1992; 8:107–115. [PubMed: 1730003]

- Ruchhoeft ML, Ohnuma S, McNeill L, Holt CE, Harris WA. The neuronal architecture of *Xenopus* retinal ganglion cells is sculpted by rho-family GTPases in vivo. *J. Neurosci.* 1999; 19:8454–8463. [PubMed: 10493746]
- Ruthazer ES, Cline HT. Insights into activity-dependent map formation from the retinotectal system: a middle-of-the-brain perspective. *J. Neurobiol.* 2004; 59:134–146. [PubMed: 15007832]
- Sabry JH, O'Connor TP, Evans L, Toroian-Raymond A, Kirschner M, Bentley D. Microtubule behavior during guidance of pioneer neuron growth cones in situ. *J. Cell Biol.* 1991; 115:381–395. [PubMed: 1918146]
- Salazar MA, Kwiatkowski AV, Pellegrini L, Cestra G, Butler MH, Rossman KL, Serna DM, Sondak J, Gertler FB, De Camilli P. Tuba, a novel protein containing bin/amphiphysin/Rvs and Dbl homology domains, links dynamin to regulation of the actin cytoskeleton. *J. Biol. Chem.* 2003; 278:49031–49043. [PubMed: 14506234]
- Schaefer AW, Kabir N, Forscher P. Filopodia and actin arcs guide the assembly and transport of two populations of microtubules with unique dynamic parameters in neuronal growth cones. *J. Cell Biol.* 2002; 158:139–152. [PubMed: 12105186]
- Sin WC, Haas K, Ruthazer ES, Cline HT. Dendrite growth increased by visual activity requires NMDA receptor and Rho GTPases. *Nature.* 2002; 419:475–480. [PubMed: 12368855]
- Skoble J, Auerbuch V, Goley ED, Welch MD, Portnoy DA. Pivotal role of VASP in Arp2/3 complex-mediated actin nucleation, actin branch-formation, and *Listeria monocytogenes* motility. *J. Cell Biol.* 2001; 155:89–100. [PubMed: 11581288]
- Tanaka E, Sabry J. Making the connection: cytoskeletal rearrangements during growth cone guidance. *Cell.* 1995; 83:171–176. [PubMed: 7585934]
- Taunton J, Rowning BA, Coughlin ML, Wu M, Moon RT, Mitchison TJ, Larabell CA. Actin-dependent propulsion of endosomes and lysosomes by recruitment of N-WASP. *J. Cell Biol.* 2000; 148:519–530. [PubMed: 10662777]
- Tessier-Lavigne M, Goodman CS. The molecular biology of axon guidance. *Science.* 1996; 274:1123–1133. [PubMed: 8895455]
- van Horck FP, Weill C, Holt CE. Retinal axon guidance: novel mechanisms for steering. *Curr. Opin. Neurobiol.* 2004; 14:61–66. [PubMed: 15018939]
- Walders-Harbeck B, Khaitlina SY, Hinssen H, Jockusch BM, Illenberger S. The vasodilator-stimulated phosphoprotein promotes actin polymerisation through direct binding to monomeric actin. *FEBS Lett.* 2002; 529:275–280. [PubMed: 12372613]
- Wanner SJ, Danos MC, Lohr JL, Miller JR. Molecular cloning and expression of Ena/Vasp-like (Evl) during *Xenopus* development. *Gene Expr. Patterns.* 2005; 5:423–428. [PubMed: 15661649]
- Wills Z, Bateman J, Corey CA, Comer A, Van Vactor D. The tyrosine kinase Abl and its substrate enabled collaborate with the receptor phosphatase Dlar to control motor axon guidance. *Neuron.* 1999; 22:301–312. [PubMed: 10069336]
- Witte S, Stier H, Cline HT. In vivo observations of timecourse and distribution of morphological dynamics in *Xenopus* retinotectal axon arbors. *J. Neurobiol.* 1996; 31:219–234. [PubMed: 8885202]
- Xanthos JB, Wanner SJ, Miller JR. Cloning and developmental expression of *Xenopus* Enabled (Xena). *Dev. Dyn.* 2005; 233:631–637. [PubMed: 15778995]
- Yu TW, Bargmann CI. Dynamic regulation of axon guidance. *Nat. Neurosci.* 2001; 4:1169–1176. [PubMed: 11687826]
- Yu TW, Hao JC, Lim W, Tessier-Lavigne M, Bargmann CI. Shared receptors in axon guidance: SAX-3/Robo signals via UNC-34/Enabled and a Netrin-independent UNC-40/DCC function. *Nat. Neurosci.* 2002; 5:1147–1154. [PubMed: 12379860]
- Zheng JQ, Wan JJ, Poo MM. Essential role of filopodia in chemotropic turning of nerve growth cone induced by a glutamate gradient. *J. Neurosci.* 1996; 16:1140–1149. [PubMed: 8558243]
- Zhou FQ, Waterman-Storer CM, Cohan CS. Focal loss of actin bundles causes microtubule redistribution and growth cone turning. *J. Cell Biol.* 2002; 157:839–849. [PubMed: 12034775]

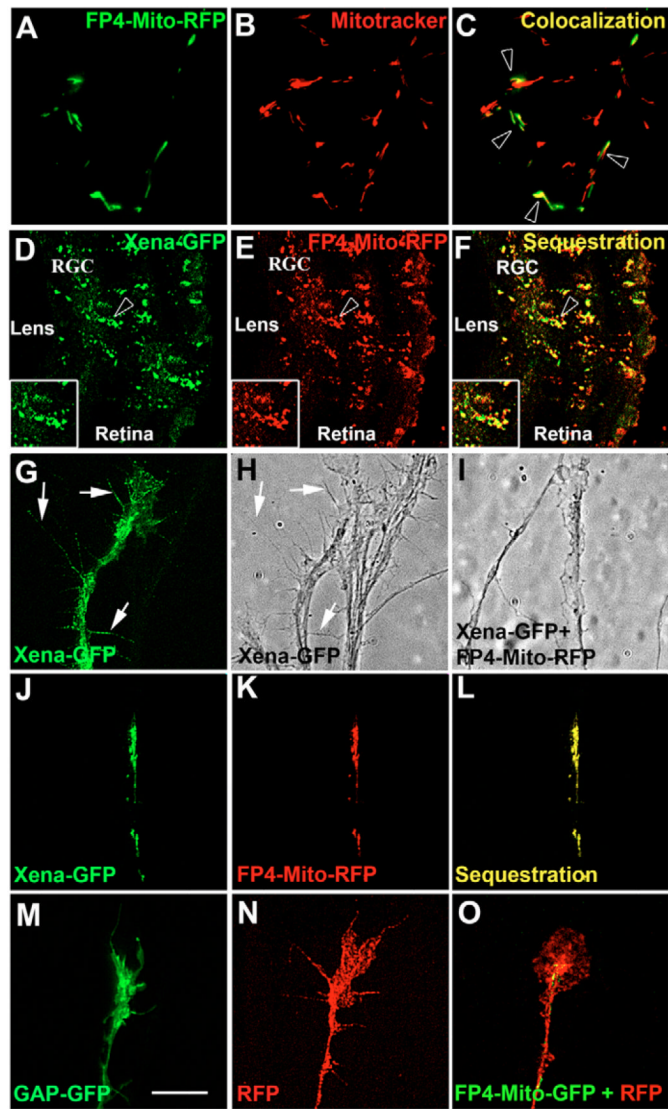


Fig. 1. Sequestration of Xena after the expression of mitochondria-binding Ena/VASP proteins and its effects on growth cone morphology
 (A-C) FP4-Mito-GFP (green, A) colocalized with the mitotracker (red, B) in retinal axons (arrowheads, C). (D-F) Xena-GFP (green, D) colocalized with FP4-Mito-RFP (red, E) in retinal cells co-expressing both constructs (F) in cryostat sections of stage 42 eyes. Arrowheads show the regions in the inserts. Inserts highlight the sequestration of Xena by the Mito construct. (G,H) In a stage 39 retinal explant, Xena-GFP was enriched along the retinal axon shaft and at the tips of growth cone filopodia (arrows). (H) Phase-contrast picture of G. (I) Phase-contrast picture of J-L. (J-L) Expression of the FP4-Mito construct (red, K) selectively depleted Xena-GFP (green, J) from sites of normal localization and sequestered it on the mitochondrial surface (L). (K) RFP-labeled mitochondria in a retinal axon expressing FP4-Mito-RFP. (M-O) Growth cone morphology of control GAP-GFP-labeled (M), control RFP-labeled (N) or FP4-Mito-GFP+RFP-labeled inactivated (O) retinal ganglion cells (RGCs) in explant culture. RGC, retinal ganglion cells. Scale bar: 56 μ m in M for D-F; 8.5 μ m in M for A-C,G-O.

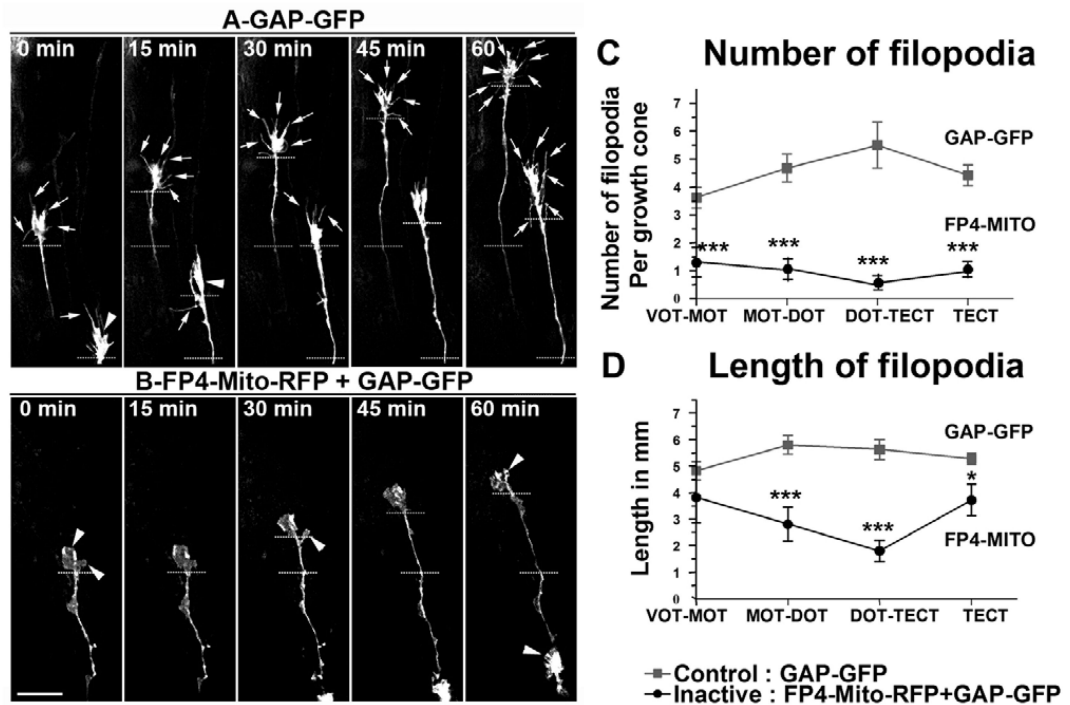


Fig. 2. Depletion of Xena/XVASP function affects growth cone dynamics in vivo
(A,B) In vivo time-lapse sequences over 1 hour (sequential pictures taken at 15-minute intervals) of growth cones growing along the optic tract of control neurons expressing GAP-GFP **(A)** or FP4-Mito-RFP+GAP-GFP-expressing neurons **(B)**. Arrows point to filopodia and arrowheads to lamellipodia; dashed lines indicate growth cone progression between sequential pictures. **(C,D)** The number of filopodia **(C)** and the length of filopodia **(D)** of retinal axon growth cones expressing either GAP-GFP or FP4-Mito (mean±s.e.m. from a sample of 15 retinal axons). Measurements were performed along the visual pathway: from the ventral to the medial optic tract (VOT-MOT), from the medial to the dorsal optic tract (MOT-DOT), at the tectum border (DOT-TECT) and inside the tectum (TECT). * $P < 0.05$; *** $P < 0.001$, FP4-Mito-expressing growth cones compared with control growth cones in corresponding segments of the visual pathway. Scale bar: 22 μm in B for A,B.

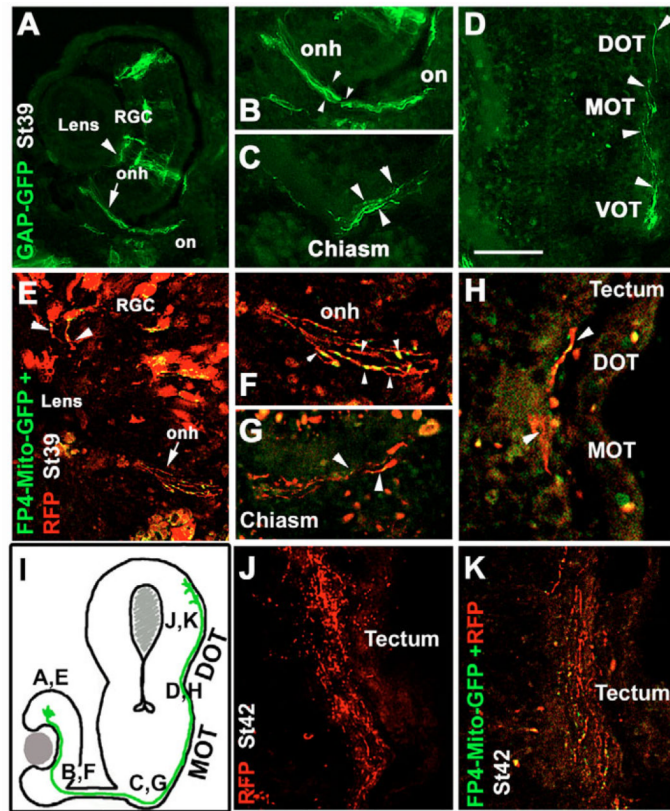


Fig. 3. Depletion of Xena/XVASP function interferes with the elongation but not with the guidance of retinal ganglion cell axons

Retinal ganglion cell (RGC) axon growth and guidance were analyzed in serial coronal cryostat sections at stage 39 (A-H) and stage 42 (J,K). RGCs expressed the control constructs GAP-GFP (A-D) or RFP (J), or the combined FP4-Mito-GFP+RFP constructs (E-H,K). (I) Drawing representing the stereotypical route followed by RGC axons during development and indicating the regions illustrated in A-H,J,K. (A-H) Arrowheads outline individual axons. (A,B) Axons of control RGCs exit the eye through the optic nerve head (onh; arrow in A). (B) Closeup of A. (C,D) The fibers navigate contralaterally across the optic chiasm, and cross the ventral (VOT), the medial (MOT) and the dorsal (DOT) optic tract to reach the tectum. (E-H) At stage 39, axons of RGCs expressing FP4-Mito initiate (arrowheads in E) and develop normally inside the optic nerve head (F and arrow in E), but only very few axons were detected at the level of the optic chiasm (G) and of the optic tract (H). (J,K) At stage 42, as in controls, the majority of RGC axon terminals of neurons expressing FP4-Mito had reached the tectum. on, optic nerve; onh, optic nerve head; RGC, retinal ganglion cell; DOT/MOT/VOT, dorsal/medial/ventral optic tract, respectively. Scale bar: 120 μ m in A,D,E,J,K; 60 μ m in B,C; 40 μ m in F-H.

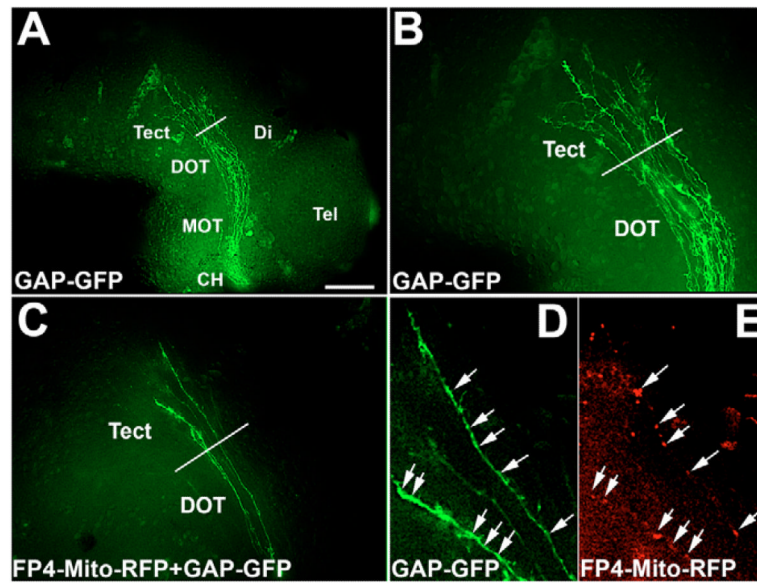


Fig. 4. Function of the Xena/XVASP proteins is not required for axon pathfinding in the optic tract

(A-E) Lateral views of stage 39 whole-mount brains illustrating the axons of control GAP-GFP-expressing (A,B) and FP4-Mito-RFP+GAP-GFP-expressing (C-E) RGC neurons. The solid line approximates the location of the rostral border of the tectum. (A,B) Control axons labeled with GAP-GFP grew in the medial and dorsal optic tracts (MOT and DOT, respectively), turned caudally in the mid-diencephalon (Di) and penetrated into the tectum (Tect), where they arborized. (C) Axons of neurons expressing FP4-Mito navigated correctly. However, only very few retinal axons with impaired function of the Xena/XVASP proteins were detected in the optic tract or in the tectum. (D,E) We confirmed that the GAP-GFP axons in D expressed the Mito construct by detecting the presence of FP4-Mito-RFP on the mitochondria (E; arrows). CH, optic chiasm; Di, mid-diencephalon; DOT/MOT/VOT, dorsal/medial/ventral optic tract, respectively; Tect, tectum; Tel, telencephalon. Scale bar: 84 μ m in A; 42 μ m in A for B,C; 30 μ m in A for D-E.

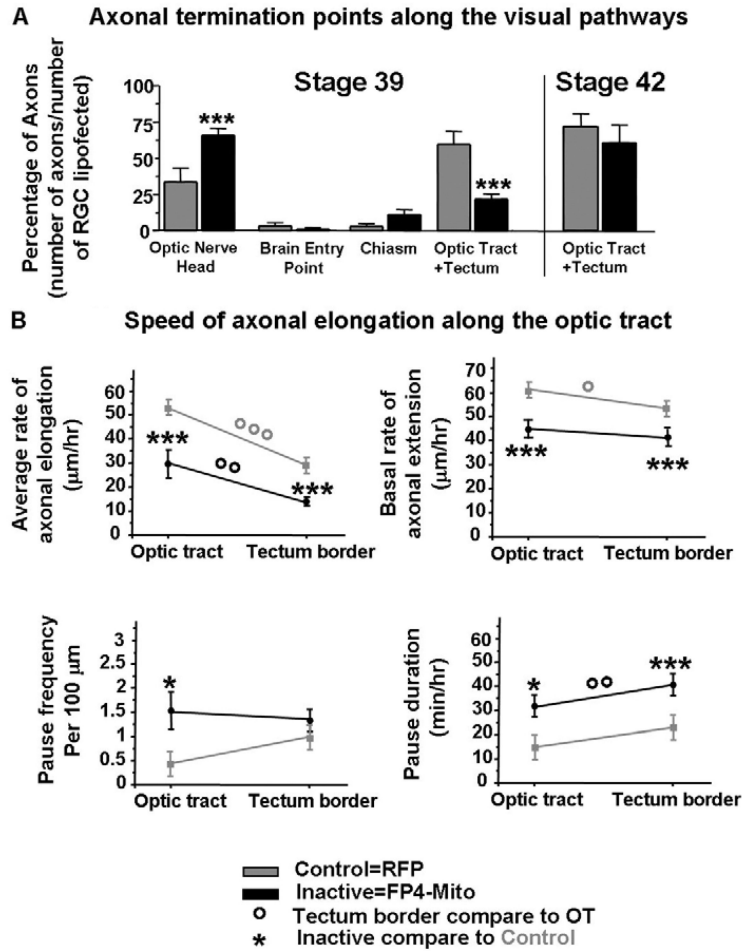


Fig. 5. Retinal ganglion cell axonal outgrowth is slower after the depletion of the Xena/XVASP proteins

(A) The percentage of retinal axons, lipofected with control RFP or with FP4-Mito-GFP +RFP, with terminals in the optic nerve head, the brain entry point, the optic chiasm or the optic tract and tectum at stage 39 (left) and with terminals in the optic tract and tectum at stage 42 (right) [mean±s.e.m. from samples of 120 retinal ganglion cells (RGCs)]. *** $P < 0.001$, FP4-Mito-expressing growth cones compared with control growth cones in the corresponding region. (B) The average rate of elongation, basal rate of extension, frequency and duration of growth cone pauses from the ventral to the dorsal optic tract (VOT-DOT), as well as at the tectum border, are shown (mean±s.e.m. from samples of 15 RGCs). * $P < 0.05$, *** $P < 0.001$; FP4-Mito-expressing growth cones compared with control growth cones in similar portions of the optic tract. ° $P < 0.05$, °° $P < 0.01$, °°° $P < 0.001$, compared axons in the optic tract and at the tectum border. OT, optic tract; RGCs, retinal ganglion cells.

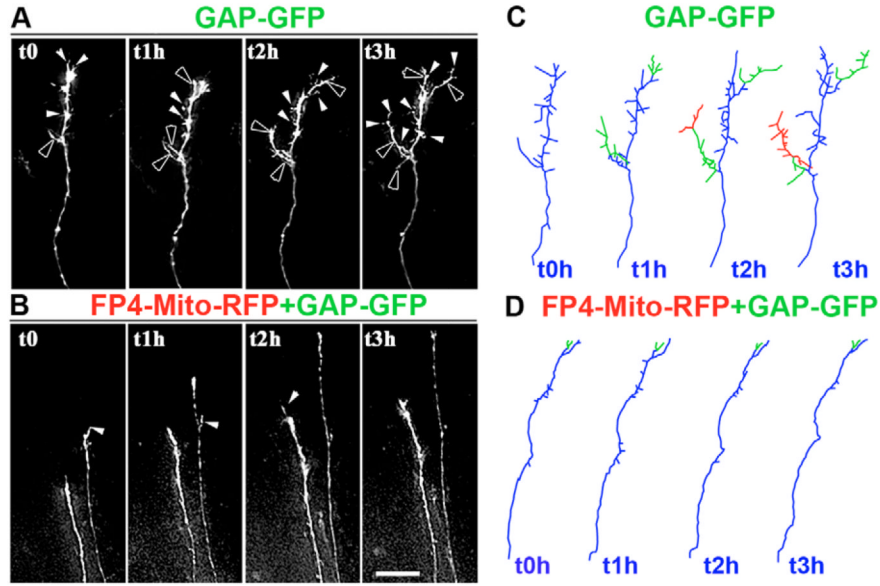


Fig. 6. Retinal axons with impaired activity of the Xena/XVASP proteins generated a limited number of filopodia-like processes and only rarely a few branches
(A,B) In vivo time-lapse sequences of terminal arborizations of control GAP-GFP-expressing (A) and of FP4-Mito-RFP+GAP-GFP-expressing (B) retinal ganglion cell (RGC) neurons in the tectum. Growth cones were photographed every hour during the 3 hours following the entry of retinal axons in the tectum. White arrowheads point to growth cone filopodia and black arrowheads to branches. (C,D) Diagrams of control GAP-GFP-expressing (C) and FP4-Mito-RFP+GAP-GFP-expressing (D) axonal terminal arborizations. Primary (blue), secondary (green) and tertiary (red) branch segments are illustrated. Scale bar: 32 μ m in B for A,B.

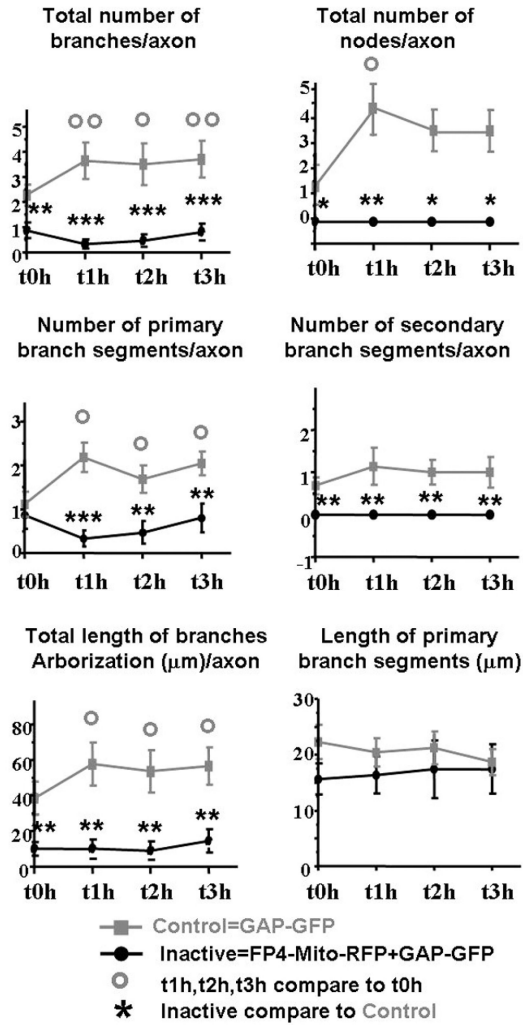


Fig. 7. Activity of the Xena/XVASP proteins controls the formation of branches at retinal axon terminals

Branching parameters in control GAP-GFP-expressing and FP4-Mito-RFP+GAP-GFP-expressing neurons. The total number of branches, the total number of nodes, the number of primary and secondary branches, the length of primary branch segments, and the length of the total arborization are shown at the time of tectum entry (t0h, or at 1, 2 and 3 hours (t1h, t2h and t3h, respectively) after the retinal ganglion cell (RGC) axons have invaded the tectum (mean±s.e.m. from a sample of 20 retinal axons). * P <0.05, ** P <0.01 and *** P <0.001, FP4-Mito-expressing axons compared with corresponding control axons. ° P <0.05 and °° P <0.01, axons at 1, 2 and 3 hours compared with axons at 0 hours.